

Altered alveolar mechanics in the acutely injured lung

Henry J. Schiller, MD; Ulysse G. McCann II, MD; David E. Carney, MD; Louis A. Gatto, PhD;
Jay M. Steinberg, DO; Gary F. Nieman, BA

Objectives: Alterations in alveolar mechanics (i.e., the dynamic change in alveolar size during tidal ventilation) are thought to play a critical role in acute lung injuries such as acute respiratory distress syndrome (ARDS). In this study, we describe and quantify the dynamic changes in alveolar mechanics of individual alveoli in a porcine ARDS model by direct visualization using *in vivo* microscopy.

Design: Prospective, observational, controlled study.

Setting: University research laboratory.

Subjects: Ten adult pigs.

Interventions: Pigs were anesthetized and placed on mechanical ventilation, underwent a left thoracotomy, and were separated into the following two groups post hoc: a control group of instrumented animals with no lung injury ($n = 5$), and a lung injury group in which lung injury was induced by tracheal Tween instillation, causing surfactant deactivation ($n = 5$). Pulmonary and systemic hemodynamics, blood gases, lung pressures, subpleural blood flow (laser Doppler), and alveolar mechanics (*in vivo* microscopy) were measured in both groups. Alveolar size was measured at peak inspiration (I) and end expiration (E) on individual subpleural alveoli by image analysis. Histologic sections of lung tissue were taken at necropsy from the injury group.

Measurements and Main Results: In the acutely injured lung, three distinct alveolar inflation-deflation patterns were observed and classified: type I alveoli ($n = 37$) changed size minimally ($I - E\Delta = 367 \pm 88 \mu\text{m}^2$) during tidal ventilation; type II alveoli ($n = 37$) changed size dramatically ($I - E\Delta = 9326 \pm 1010 \mu\text{m}^2$) with tidal ventilation but did not totally collapse at end expiration; and type III alveoli ($n = 12$) demonstrated an even greater size change than did type II alveoli ($I - E\Delta = 15,418 \pm 1995 \mu\text{m}^2$), and were distinguished from type II in that they totally collapsed at end expiration (atelectasis) and reinflated during inspiration. We have termed the abnormal alveolar inflation pattern of type II and III alveoli "repetitive

alveolar collapse and expansion" (RACE). RACE describes all alveoli that visibly change volume with ventilation, regardless of whether these alveoli collapse totally (type III) at end expiration. Thus, the term "collapse" in RACE refers to a visibly obvious collapse of the alveolus during expiration, whether this collapse is total or partial. In the normal lung, all alveoli measured exhibited type I mechanics. Alveoli were significantly larger at peak inspiration in type II ($18,266 \pm 1317 \mu\text{m}^2$, $n = 37$) and III ($15,418 \pm 1995 \mu\text{m}^2$, $n = 12$) alveoli as compared with type I ($8214 \pm 655 \mu\text{m}^2$, $n = 37$). Tween caused a heterogenous lung injury with areas of normal alveolar mechanics adjacent to areas of abnormal alveolar mechanics. Subsequent histologic sections from normal areas exhibited no pathology, whereas lung tissue from areas with RACE mechanics demonstrated alveolar collapse, atelectasis, and leukocyte infiltration.

Conclusion: Alveolar mechanics are altered in the acutely injured lung as demonstrated by the development of alveolar instability (RACE) and the increase in alveolar size at peak inspiration. Alveolar instability varied from alveolus to alveolus in the same microscopic field and included alveoli that changed area greatly with tidal ventilation but remained patent at end expiration and those that totally collapsed and reexpanded with each breath. Thus, alterations in alveolar mechanics in the acutely injured lung are complex, and attempts to assess what may be occurring at the alveolar level from analysis of inflection points on the whole-lung pressure/volume curve are likely to be erroneous. We speculate that the mechanism of ventilator-induced lung injury may involve altered alveolar mechanics, specifically RACE and alveolar overdistension. (*Crit Care Med* 2001; 29:1049-1055)

KEY WORDS: lung; *in vivo* microscopy; alveoli; respiratory distress syndrome; mechanical ventilation; pulmonary surfactant; alveolar mechanics; respiratory mechanics; volutrauma; alveolar recruitment-derecruitment

Positive pressure mechanical ventilation has remained a mainstay for the support and treatment of acute lung injury and acute respiratory distress syndrome (ARDS) for over 40 yrs (1). More recently,

it has been recognized that, in addition to providing ventilatory support, mechanical ventilation may induce a lung injury clinically indistinguishable from ARDS (1). Ventilator-induced lung injury (VILI) occurs in 5% to 38% of all mechanically ventilated patients (2) and carries a mortality of 13% to 35% (3). Furthermore, it is possible that VILI may exacerbate and perpetuate the systemic inflammatory response that is the cause of ARDS and multiple organ system failure (4).

A current hypothesis implicates alveolar shear stress, secondary to alveolar recruitment-derecruitment, as the mechanism of VILI (5-8). However, evidence supporting this hypothesis is inferential,

based on indirect measurements such as whole-lung pressure-volume tracings and computerized tomographic images (5-8). Alveolar recruitment-derecruitment has never been directly observed or confirmed. Using *in vivo* videomicroscopy, we directly observed and quantified alveolar mechanics (i.e., the dynamic changes in alveolar size throughout the ventilatory cycle) during tidal ventilation in the normal and acutely injured lung. These studies demonstrated that normal alveoli, once recruited, do not change volume appreciably during tidal ventilation (9). However, following surfactant deactivation, which is a hallmark of ARDS, we observed markedly abnormal

From the Department of Surgery, SUNY Health Science Center, Syracuse, NY (HJS, UGM, DEC, JMS, GFN); and the Department of Biology, Cortland College, Cortland, NY (LAG).

Supported, in part, by a SUNY Upstate Medical University Intramural Grant (Hendricks Fund: 211-0128A). The Amadeus[®] Ventilator was donated by Hamilton Medical Inc.

Address requests for reprints to: Gary F. Nieman, BA, SUNY Upstate Medical University, Department of Surgery, 750 E. Adams Street, Syracuse, NY 13210.

Copyright © 2001 by Lippincott Williams & Wilkins

alveolar mechanics characterized by repetitive alveolar collapse and expansion (10). This pathologic form of alveolar mechanics, which we refer to by the acronym RACE, is a much more complex process and distinctly different from simple recruitment-derecruitment. This complex array of alveolar mechanics includes a type of alveoli that changes volume imperceptibly with ventilation (i.e., normal alveoli), a type that changes volume significantly with ventilation but does not collapse at end expiration, and a type of alveoli that totally collapses and reinflates with each breath. Our data demonstrate that acute lung injury results in a continuum of abnormal alveolar mechanics that may cause significant shear stress-induced lung injury and play a major role in the development of VILI.

Only three previous studies have used *in vivo* microscopy to study normal alveolar mechanics (11–13). To our knowledge, we are the only group using *in vivo* microscopy in the study of *abnormal* alveolar mechanics (10, 14, 15). We propose a classification scheme to describe abnormal alveolar mechanics with the intent of providing a tool to facilitate future studies in the pathophysiology of VILI and the development of future strategies to prevent VILI.

METHODS AND MATERIALS

Anesthetized Yorkshire pigs weighing 18–33 kg were pretreated with atropine (0.05 mg/kg intramuscularly [im]) 10–15 mins before intubation, and were preanesthetized with ketamine (30 mg/kg im) and xylazine (2 mg/kg im). Intravenous sodium pentobarbital (6 mg/kg/hr) was delivered via a Harvard infusion pump (model 907, Harvard Apparatus, Mills, MA) and was used for continuous anesthesia (6 mg/kg/hr). The animals were ventilated with 50% oxygen delivered via an Amadeus^{FT} ventilator (Hamilton Medical, Reno, NV). Tidal volume was set at 10 mL/kg, with 2 cm H₂O positive end-expiratory pressure and respiratory rate titrated to a minute volume of 4.0 L/min. A left carotid artery cutdown was established with 2-mm inside diameter polyethylene tubing for blood gas measurements (Model ABL5, Radiometer Medical A/S, Copenhagen, Denmark), blood oxygen content analysis (Model OSM3, Radiometer Medical A/S), and systemic arterial pressure monitoring. A 7-Fr flow-directed Swan-Ganz thermodilution catheter was passed through the left femoral vein into the pulmonary artery for pulmonary artery, pulmonary artery wedge, and central venous pressure measurements, mixed venous blood gas and O₂ content sampling, and with

cardiac output (CO) and lung function determinations (Baxter Explorer, Edwards Critical Care, Irvine, CA). CO measurements were made in duplicate at end expiration. A triple-lumen catheter was placed into the jugular vein for fluid, anesthesia, and drug infusion. Pressures were measured using transducers (Argon Model 049-992-000A, CB Sciences Inc., Dover, NH) leveled with the right atrium and recorded on a 16-channel PowerLab/16s (AD Instruments Pty. Ltd., Milford, MA) and a Dell Dimension (Model XPS R400, Dell, Inc., Dallas, TX) computer. Cardiac rhythm was measured with a Zoll pacemaker-defibrillator (Zoll Medical, Burlington, MA). A left thoracotomy was established through the fifth intercostal space, and the fifth rib was removed.

Ventilator parameters measured included peak airway pressure, plateau pressure, and pulmonary compliance, all measured and calculated by the Amadeus^{FT} ventilator. Peak airway pressure, by definition, was the highest airway pressure measured during inspiration, plateau pressure was measured following an inspiratory pause of 5% of the total inspiratory time, and static compliance was calculated by dividing the plateau pressure by the tidal volume measured by the expiratory flow sensor.

Acute Lung Injury. Tween instillation is an established model to deactivate pulmonary surfactant and cause immediate lung injury (10). After surgery, pigs were placed on their left side and a 5% solution of Tween 20 in saline (3 mL/kg) was instilled into the lung. The instilled fluid was injected through a 2-mm inside diameter catheter that was threaded through the endotracheal tube to the tracheal bifurcation and directed to the dependent lung. After injection of the solution, the endotracheal tube was reconnected to the ventilator, and three deep sighs (two times the tidal volume) were delivered. The endotracheal tube was then suctioned free from residual fluid and the pigs were rotated to their right side for attachment of the videomicroscope. Control animals were treated in a similar fashion but without Tween 20 instillation. We previously identified the structures measured to be true alveoli and have demonstrated that saline instillation without Tween 20 does not alter alveolar mechanics (10).

In vivo Microscopy. Our technique of *in vivo* microscopy has been described in detail elsewhere (10, 16). Briefly, the *in vivo* microscope (epiobjective metallurgic microscope with dark field illumination, Wild-Heerbrugg, Switzerland) with coverslip suction head apparatus was brought into place on the lateral aspect of the left diaphragmatic lobe through the thoracotomy and suction was applied (≤ 5 cm H₂O) at end inspiration to affix the lung in place. Suction was minimal to ensure lung stability without altering alveolar mechanics (10). The microscopic images were viewed with a video camera (Model CCD SSC-S20, SONY Inc., Pitman, NJ), recorded with a video

recorder (Model SVO-9500 MD, SONY Inc.), and analyzed with a computerized image analysis system (Version 4.1 Image ProTMPlus, Media Cybernetics, Silver Spring, MD). Continuous filming of individual alveoli was performed throughout five complete tidal ventilations for alveolar mechanics analysis. Subpleural blood flow was measured with a laser Doppler flow probe (Type P, Transonic Systems, Inc., Ithaca, NY) and recorded with laser Doppler flow meter (ALF-21, Transonic Systems, Inc.). The laser probe chosen used a 740-nm wavelength with a distance between transmitter and receiver of 0.5 mm to produce a signal penetration of 1 mm³. The suction head apparatus was adapted to accommodate the laser flow probe so that pulmonary microvascular blood flow could be measured in close proximity (~ 2 cm) to the area on the lung used to measure alveoli mechanics.

Protocol. Pigs were randomly divided into the following two groups: a control group (n = 5) of instrumented animals with no lung injury, and an acute lung injury group (n = 5), with Tween instillation into the animals lungs. After surgical preparation, the suction-coverslip apparatus was attached to the lung and the microscope was focused on the subpleural alveoli. Tween instillation caused a heterogenous injury such that there were obvious injured areas on the lung surface. Because the specific aim of this study was to identify abnormal alveolar mechanics, we selected only the injured areas to film in Tween-exposed lungs. Control lung had a homogeneous, normal-appearing lung surface.

Our *in vivo* microscopic technique allowed us to film the same alveolus continually throughout tidal ventilation (9–11). Alveoli were noted to have different inflation patterns in the Tween-injured compared with the normal control lung. We were able to describe the following three broad types of alveolar mechanics based solely on visual observations. Type I alveoli demonstrate no visible change in size and/or shape with tidal ventilation. Type II alveoli visibly change size and shape with ventilation but do not totally collapse at end expiration. Type III alveoli, which totally collapse at end expiration, “pop” open and rapidly increase in size with inspiration and then collapse during expiration.

All alveoli in the control animals were type I and, therefore, represent normal alveolar mechanics, a finding consistent with previous studies (9). Type II and III mechanics were never seen in normal lungs and, therefore, type II and III alveoli represent abnormal alveolar mechanics and were selected from Tween-instilled lungs. Once alveoli had been visually classified according to type, they were filmed for subsequent measurement of alveolar area at end expiration and peak inspiration using image analysis. Alveolar area in type I (n = 37), type II (n = 37), and type III (n = 12) alveoli were analyzed. Fewer type III alveoli were analyzed inasmuch as they were fewer in number than types I and II.

Image Analysis. Continuous filming of individual alveoli was performed throughout five complete tidal ventilations. Still images were obtained from these films at peak inspiration and end expiration and analyzed by the computer. The image field was calibrated with a micrometer. To assure unbiased outlines, images were unlabeled and randomly analyzed in terms of expiration or inspiration. The change in alveolar area between inspiration and expiration ($I - E\Delta$) was calculated on a standard data spreadsheet (Microsoft Excel) and expressed as mean \pm SE. We have previously performed calculations to derive alveolar volume from alveolar area measurements (9). This required the assumption of a three-dimensional unbiased linear change in direction. Although this assumption may be valid in type I alveoli, we have observed asymmetric

changes in area with type II and III alveoli. Therefore, alveoli undergoing RACE do not necessarily change directions equally in three dimensions. We subsequently report our results as area rather than a calculated volume.

Histology. At necropsy, a 1-cm³ section of lung was cut from a lung area with either normal or RACE alveolar mechanics in the acute lung injury group. The type of alveolar mechanics was confirmed with the *in vivo* microscope immediately before the animal was killed and was marked with a tissue marker. The normal and RACE areas selected for presentation (Fig. 1) were within 2 cm of each other. All lung samples were harvested and fixed at atmospheric pressure after lung inflation to a volume equal to two tidal volumes to standardize the volume history. The lung sample was placed in 10% buffered for-

malin and prepared for standard hematoxylin and eosin staining.

Vertebrate Animals. Experiments described in this study were performed in adherence with the National Institutes of Health guidelines for the use of experimental animals in research. The protocol was approved by the Committee for the Humane Use of Animals at our institution.

Statistics. Significant differences between the control and acute lung injury groups in hemodynamic and blood chemistry parameters were determined using an unpaired Student's *t*-test. The differences in $I - E\Delta$ and absolute alveolar area between the three alveolar mechanics types were determined by a one-way analysis of variance. Whenever the *F* ratio indicated a significant difference, a Newman-Keuls post hoc test was used to identify the individual differences. Significance was assumed if the probability of the null hypothesis was $<5\%$ ($p < 0.05$).

RESULTS

The histology of lung areas with normal and RACE alveolar mechanics is seen in Figure 1. These lung areas were located within 2 cm of each other along the lung surface. The area with normal alveolar mechanics (Fig. 1A) has fully inflated alveoli with thin alveolar walls and no apparent infiltration of leukocytes. In the area with RACE mechanics (Fig. 1B), alveoli are reduced in volume or collapsed (atelectasis) and have thickened alveolar walls. Also, a large number of leukocytes have sequestered in the pulmonary parenchyma.

Photomicrographs of the three types of alveolar mechanics, captured by *in vivo* microscope, are depicted in Figure 2. For each type, the same alveolus (outlined by white dots) is pictured at end expiration and at peak inspiration. We were able to visually classify the alveolar mechanics observed into three types. Type I alveoli do not visibly change size or shape during tidal ventilation. The normal lung is composed almost exclusively of type I alveoli, which confirms our earlier interpretations (9, 10). After Tween 20 instillation, alveolar mechanics become much more complex, with all three alveolar mechanics types present. Type II alveoli exhibit obvious changes in both alveolar size and shape during tidal ventilation. However, the alveolus does not completely collapse at end expiration (Fig. 2C). In contrast, type III alveoli totally collapse at end expiration (Fig. 2E) and "pop" open during inspiration, becoming fully inflated at peak inspiration (Fig. 2F).

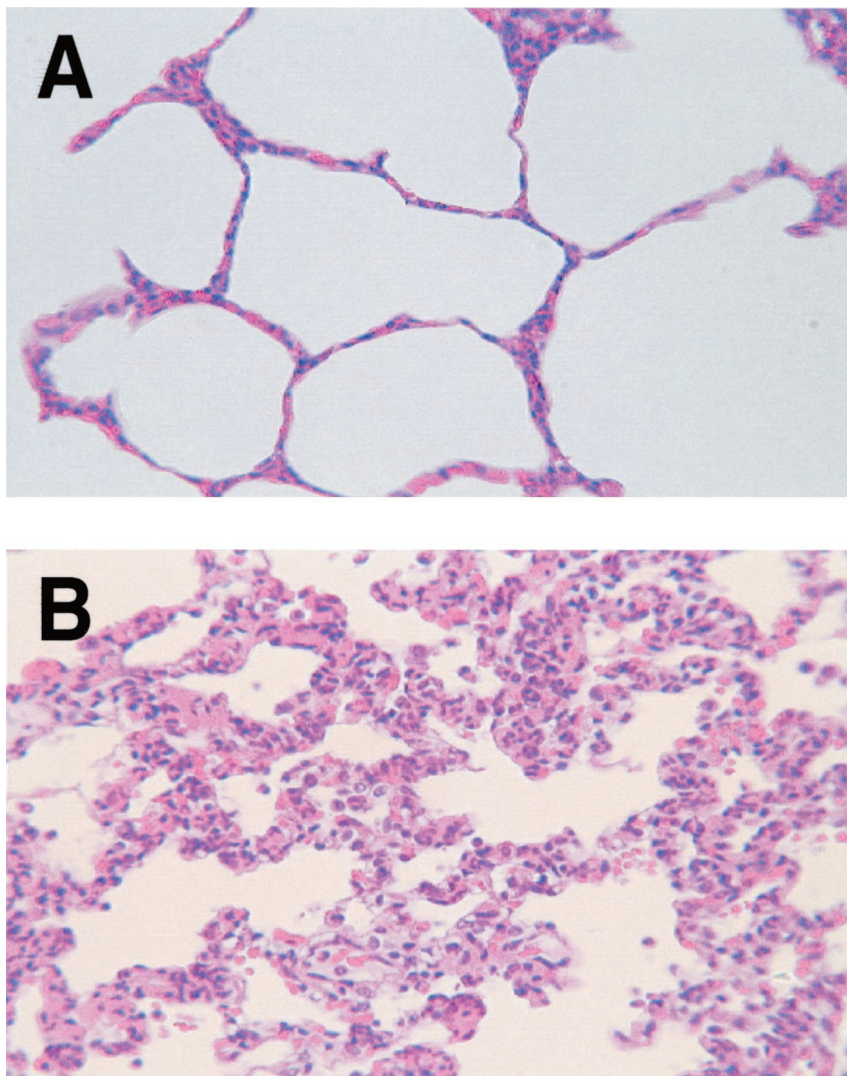


Figure 1. Histologic sections of lung from normal (A) and repetitive alveolar collapse and expansion (RACE) (B) areas of lung after surfactant deactivation. The presence of normal or RACE mechanics was confirmed using *in vivo* microscopy. The lung sections selected for sampling were within 2 cm of each other. Note normal alveolar aeration and the lack of sequestered leukocytes in lung areas with normal alveolar mechanics (A). Lung areas with RACE mechanics (B) demonstrated atelectasis and a significant leukocyte infiltration typical of acute lung injuries.

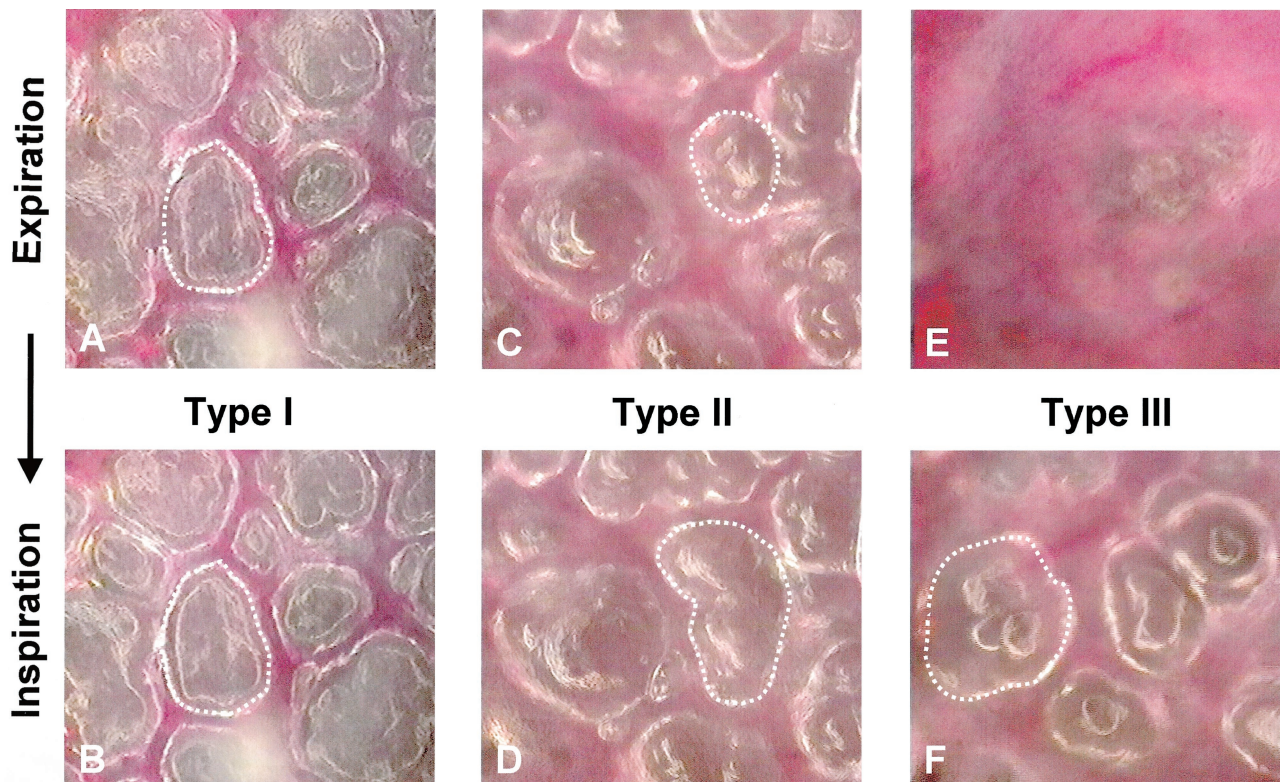


Figure 2. Photomicrographs depicting individual alveoli as they are inflated from end expiration (*Expiration*) to peak inspiration (*Inspiration*) during tidal ventilation in the acutely injured lung (Tween lavage). Alveoli of interest have been highlighted with white dots and represent the same alveolus at expiration and inspiration. Alveolar inflation patterns were separated into three types depending on the appearance of alveolar area changes with tidal ventilation. Type I alveoli change volume imperceptibly from end expiration (A) to peak inspiration (B). Type II alveoli change volume from end expiration (C) to peak inspiration (D) but stay inflated at end expiration. Type III alveoli collapse totally at end expiration (E) and re-inflate with inspiration (F). In the normal lung, all alveoli exhibit type I inflation patterns (15).

The change in alveolar area from peak inspiration to end expiration ($I - E\Delta$) in the three visually identifiable alveolar mechanic types is depicted in Figure 3. Morphometric analysis demonstrated that type I alveoli change area very little during tidal ventilation, confirming our visual impressions. In contrast, both type II and III alveoli demonstrate larger changes in area from expiration to inspiration than do type I alveoli (Fig. 3). The $I - E\Delta$ of type III alveoli was greater than that of type II alveoli (Fig. 3).

Figure 4 depicts mean alveolar cross-sectional area (μm^2) at both peak inspiration and end expiration in all three alveolar types. Alveolar size is similar at inspiration and expiration in the type I alveoli, confirming the visual impression of imperceptible area change with this alveolar type. After surfactant deactivation, there was little difference in alveolar size at end expiration between type I and II alveoli. End expiratory volume was always zero in type III alveoli inasmuch as they are atelectatic by definition. There was, however, a large increase in inspira-

tory area in both type II and type III alveoli as compared with type I.

Table 1 summarizes the hemodynamic and blood chemistry data. Measurements were made during the filming of alveoli before (control) and after surfactant deactivation (Tween). As expected, Tween instillation caused a significant fall in both dynamic and static pulmonary compliance, and both peak and plateau airway pressures were significantly increased. Decreased compliance was associated with a significant fall in arterial PO_2 and a marked rise in pulmonary shunt fraction. Pulmonary microvascular blood flow, measured by laser Doppler, was not altered by Tween instillation.

DISCUSSION

Our data are consistent with our previous findings and demonstrate that normal lung volume change is not associated with linear, balloonlike expansion and contraction of alveoli throughout tidal ventilation (9). Rather, alveolar area, and therefore alveolar volume, appears to be

remarkably unchanged throughout the respiratory cycle, suggesting that the majority of lung volume change seen with tidal ventilation is due either to recruitment-derecruitment or to change in vol-

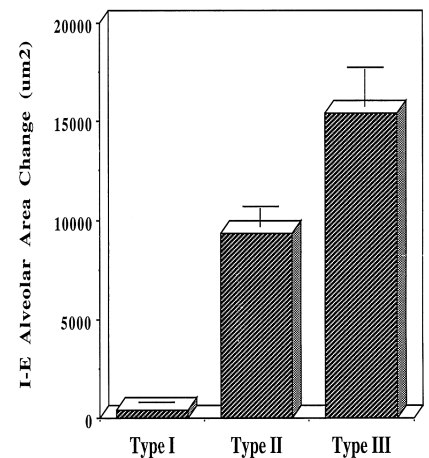


Figure 3. The peak inspiratory (I) to end expiratory (E) change in alveolar area during tidal ventilation in the three types of alveolar inflation patterns. Data are mean \pm SE.

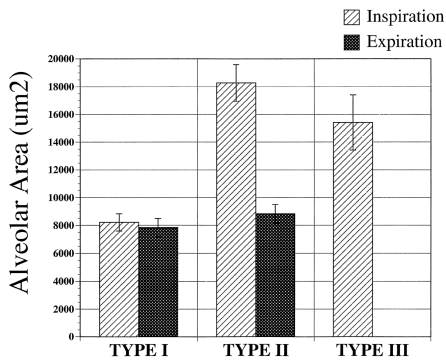


Figure 4. Absolute alveolar size expressed as alveolar cross-sectional area in all three alveolar types at both peak inspiration and end expiration. Alveolar area at peak inspiration was significantly greater in type II and III alveoli as compared with type I, confirming our visual impressions. There were no differences in alveolar cross-sectional area at end expiration between type I and II alveoli. Alveolar volume at end expiration in type III alveoli was zero by definition. Data are mean \pm SEM.

ume in the conducting airways of the lung (9). Further, it demonstrates that a continuum of abnormal alveolar mechanics is triggered after surfactant deactivation. In this initial analysis, we describe three types of alveolar mechanics—normal (type I) and abnormal (types II and III)—based on the presence of a visually perceptible change in alveolar size with tidal ventilation and whether abnormal alveoli become atelectatic at end expiration. We have confirmed our visual

impressions with an objective determinant of inspiratory-to-expiratory area change ($I - E\Delta$).

In addition to the increased $I - E\Delta$ associated with abnormal alveolar mechanics, the absolute size of the alveolus is significantly increased at peak inspiration. The increases in both absolute alveolar size and $I - E\Delta$ measured in RACE areas are associated with histologic changes of atelectasis and leukocyte infiltration typical of acute lung injury (Fig. 1). In previous studies, we demonstrated that tidal volumes as high as 30 mL/kg did not increase alveolar size at peak inspiration in normal lungs (17). However, in acutely injured lungs, alveolar size at peak inspiration is doubled (Fig. 4) compared with normal alveoli even with a normal tidal volume (10 mL/kg). We speculate that heterogenous atelectasis causes patent alveoli to overinflate by “bulging” into the space vacated by the collapsed alveoli. Taken together, our *in vivo* data suggest that alveolar overexpansion (volutrauma) does not occur in the normal lung (17) but may occur after heterogeneous surfactant deactivation.

Pathophysiologic Consequence of Abnormal Alveolar Mechanics. If abnormal alveolar mechanics are indeed pathologic, the mechanism of injury must be determined. There is no doubt that abnormal alveolar mechanics have a negative impact on oxygenation, but it is less clear whether these altered alveolar infla-

tion patterns are injurious to the alveolus and surrounding microvasculature. Abnormal alveolar mechanics could cause direct mechanical injury to the alveolus and/or act as a “trigger” mechanism causing a secondary inflammatory injury. Although we quantified the increase in alveolar instability (RACE) and the increase in alveolar size at peak inspiration in this study, to thoroughly understand the dynamics of altered alveolar mechanics, the following questions must be elucidated:

Do abnormal alveoli inflate and deflate in a linear fashion throughout tidal ventilation, or is there a rapid change in size at a specific airway pressure (critical opening/closing pressure)?

At what point on the whole-lung inflation-deflation curve does alveolar size change occur?

Of the total population of alveoli, what is the fraction of each alveolar type and how does this proportion change with severity of lung injury?

Is the change in alveolar size uniform in all directions?

Do abnormal alveolar mechanics change with severity and/or model (Tween, endotoxin, oleic acid, etc.) of lung injury?

Are abnormal alveolar mechanics observed in dependent regions of the lung and does alveolar flooding of dependent alveoli influence these mechanics?

Table 1. Physiologic variables

Variable	Control (n = 5)	Tween (n = 5)	p Value
Hgb	10.9 \pm 0.7	12.4 \pm 0.8	0.2079
pH	7.2 \pm 0.03	7.1 \pm 0.02	0.0323
Po ₂	161 \pm 7.3	75.0 \pm 28.1	0.0252
Pco ₂	55.0 \pm 4.6	78.5 \pm 3.3	0.0060
HR	166 \pm 13.4	177.5 \pm 21.1	0.6617
CO	7.6 \pm 1.2	6.4 \pm 1.7	0.5851
Psys	85.5 \pm 4.7	75.5 \pm 18.6	0.0252
Ppa	25.0 \pm 3.4	30.7 \pm 2.8	0.2432
Ppw	5.2 \pm 0.8	6.6 \pm 1.6	0.4636
PVR	232.5 \pm 62	506 \pm 182	0.0551
Laser Doppler	47.8 \pm 7.3	44.2 \pm 12.7	0.8141
Shunt	16.3 \pm 1.3	61 \pm 10.4	0.0051
Pplat	20.0 \pm 1.9	27.5 \pm 2.3	0.0457
Ppeak	20.0 \pm 1.0	30.0 \pm 2.0	0.0053
Compliance	11.2 \pm 0.2	7.5 \pm 0.6	0.0011

Hgb, hemoglobin; HR, heart rate (beats/min); CO, cardiac output (L/min); Psys, systolic arterial blood pressure (mm Hg); Ppa, mean pulmonary artery pressure (mm Hg); Ppw, pulmonary wedge pressure (mm Hg); PVR, pulmonary vascular resistance (dyne \cdot sec/cm⁵); laser Doppler (mL/min/100 g); Qs/Qt, shunt fraction (%); Pplat, airway plateau pressure (cm H₂O); Ppeak, peak airway pressure (cm H₂O); Compliance (cm H₂O/mL).

Data are mean \pm SE. To convert to kPa, multiply by 0.1333.

Although, the complexities of altered alveolar mechanics require unraveling, qualitative observations in the current study suggest that a critical opening/closing pressure exists, at which time the alveolus “pops” open or closed. We have coined the term RACE to describe abnormal alveolar mechanics. RACE describes all alveoli that visibly change volume with ventilation, regardless of whether these alveoli collapse totally (type III) at end expiration. Thus, the term “collapse” in RACE refers to a visibly obvious collapse of the alveolus during expiration, whether this collapse is total or partial. The components of RACE mechanics include a large change in alveolar size (>5000 μ m² [see Fig. 3]) between inspiration and expiration and a rapid change in alveolar size over a small portion of the total inspiratory or expiratory cycle. In other words, injured alveoli do not change volume until a critical airway pressure is reached, at which time alveoli

rapidly “pop” open or closed, respectively. Thus, both type II and III alveoli fit the criteria for RACE. However, the impact of RACE on the development of VILI remains an important clinical question.

Alveolar Mechanics and Lung Injury. To understand how RACE may cause alveolar damage, the anatomy and mechanics of normal alveoli must be further investigated. Wilson and Bachofen (18) demonstrated that, once recruited, alveoli do not change volume appreciably during ventilation. Rather, lung volume changes are accommodated by expansion of the respiratory bronchiole while alveoli change from deep to shallow cups. Our group also has shown that alveoli do not change size appreciably over a wide range of lung volumes (9) and that alveolar recruitment is a normal mechanism of lung inflation (9, 19). These studies suggest that much of the change in lung volume is accommodated either by the elastic properties of the respiratory bronchiole or by the recruitment of entirely new populations of acini (9, 19). This structural design prevents shear stress injury in the normal lung inasmuch as there is little individual alveolar movement with ventilation.

Anatomically, alveoli are not separate units but are interconnected, with shared alveolar walls that attach in a cluster around a terminal bronchiole, forming an acinus. The acinus gains structural support from this anatomical arrangement, similar to the structural integrity of a honeycomb (20). Structural support, termed interdependence, combined with the surface tension–lowering properties of surfactant provide stability to alveoli such that there is little change in alveolar volume during ventilation (18, 20). However, the acinus is only structurally sound if all alveoli are inflated. Collapse of a single alveolus in an acinus causes shear stress not only on the walls of the collapsing alveolus but on the walls of all adjacent alveoli (20). If surfactant is deactivated, the shear stress that develops when an individual alveolus collapses and reopens is substantial. Calculations yield a shear stress in excess of 140 cm H₂O (20). Thus, after surfactant deactivation, the structural interdependence of the acinus is destroyed, and alveoli behave as individual “balloons,” changing volume greatly with tidal ventilation (10). We hypothesize that this dramatic alteration in alveolar mechanics exposes the alveolus to severe shear stress.

Are Direct Measurements of Abnormal Alveolar Mechanics Necessary? Numerous studies have used surrogate markers such as computerized tomography (6, 7), whole-lung pressure-volume (P/V) curves (7, 8, 21), and arterial blood gases (6, 7) to infer the effects of mechanical ventilation on alveolar mechanics. Indeed, Amato (21) inferred from whole-lung P/V curves that the lower inflection point (P_{flex}) represented alveolar recruitment and that the upper P_{flex} represented alveolar overdistension. Using only P/V curve inflection points, without direct evidence as to what these inflection points actually represent at the alveolar level, Amato designed a ventilator protocol for ARDS patients in an attempt to reduce VILI. Hickling (22), in direct opposition to Amato’s interpretation of the P/V curve, used a mathematical analysis and demonstrated that the lower P_{flex} does not necessarily represent alveolar recruitment, nor does the upper P_{flex} represent alveolar overdistension. Indeed, all of the above animal studies (6–8, 21) report alveolar recruitment-derecruitment as the mechanism that explains the changes in their measured parameters without direct confirmation that recruitment-derecruitment exists. Thus, without direct measurement of normal and pathologic alveolar mechanics and knowledge of how alveolar mechanics are affected by various ventilator modes, protective ventilator strategies will be empirical.

Critique of the Model. There are several methodologic problems with *in vivo* microscopy, yet it is the only technique available to directly visualize and measure individual alveoli throughout tidal ventilation in the living lung. The two major problems with this technique are that measurements are restricted to analysis of subpleural alveoli and only two-dimensional changes in alveolar size can be measured. Although alveoli are morphologically distinct from the visceral pleura, a concern exists that subpleural alveolar mechanics differ from those of alveoli in the lung interior secondary to pleural influences. We previously demonstrated that there is a large change in pleural surface area with minimal change in alveolar size over a wide range of lung volumes (9). If subpleural alveoli were tethered to the pleura, alveolar size change should be exaggerated with lung inflation, and yet we demonstrated very little change in alveolar size (9). Moreover, after surfactant deactivation, alveoli

demonstrate RACE mechanics with alveoli inflating and deflating at various rates and at different time points on the P/V curve, suggesting that alveoli are structurally independent of the visceral pleura rather than tethered to it (10).

Subpleural alveoli are structurally dissimilar to interior alveoli in that they are not completely surrounded by adjacent alveoli (i.e., one wall of a subpleural alveolus is adjacent to the pleura rather than shared with another alveolus). This structural arrangement may reduce the support due to alveolar interdependence, causing subpleural alveoli to collapse before those in the lung interior. However, in the classic paper by Mead (20), describing the significance of alveolar interdependence to alveolar mechanics, the model consisted of alveoli in a single plane, which is analogous to the condition of subpleural alveoli *in vivo*. Mead demonstrated that, even in a single-plane arrangement, loss of alveolar interdependence would yield shear stress in excess of 140 cm H₂O. We therefore believe that alveolar interdependence is an important structural feature in subpleural as well as centrally located alveoli.

Our technique only allows two-dimensional measurement of alveolar size (cross-sectional surface area) during ventilation. If alveoli change length (a third dimension) during ventilation, it cannot be measured due to our microscope’s limited depth of field. However, we have shown that alveolar mechanics are dramatically altered in two dimensions following surfactant deactivation. Although there may also be changes in alveolar length that are missed by our technique, we can still define and quantify normal and abnormal alveolar mechanics in two dimensions, which may be applied to a third dimensional component.

We have extensive experience with this *in vivo* microscopic technique for analyzing alveolar mechanics (9, 10, 14, 15). We have previously shown that all of the subpleural structures observed are true alveoli and that the modest suction that is applied to the pleural surface to stabilize the lung during filming does not significantly alter alveolar mechanics (9, 10, 14, 15). This study was intended as a preliminary work to establish that alveolar mechanics are significantly altered in the acutely injured lung. However, a great deal of work is necessary to accurately define all of the complexities inherent in abnormal alveolar mechanics. Future studies will investigate the presence

Although this preliminary study only defines the magnitude of abnormal alveolar size change ($I - E\Delta$) during ventilation, our observations reveal a tremendous complexity to abnormal alveolar mechanics (repetitive alveolar collapse and expansion).

of alveolar opening and closing pressures, the rate at which alveoli change size, the fraction of the various alveolar types in the injured lung, and whether abnormal alveolar mechanics change with severity of lung injury.

Summary. Although this preliminary study only defines the magnitude of abnormal alveolar size change ($I - E\Delta$) during ventilation, our observations reveal a tremendous complexity to abnormal alveolar mechanics (RACE). This study demonstrates that RACE is much more complex and distinctly different from simple recruitment-derecruitment (i.e., simple collapsing and reexpansion of alveoli during tidal ventilation). Accordingly, knowledge of normal and abnormal alveolar mechanics would seem to be fundamental to understanding the pathophysiology of VILI and, ultimately, to developing ventilator strategies to minimize it.

ACKNOWLEDGMENTS

We thank Andy Paskanik and Kathy Snyder for expert technical assistance.

REFERENCES

1. Dreyfuss D, Saumon G: Ventilator-induced lung injury: Lessons from experimental studies. *Am J Respir Crit Care Med* 1998; 157:294–323
2. Aldrich T, Present DJ: Indications for mechanical ventilation. In: Principles and Practice of Mechanical Ventilation. Tobin MJ (Ed). New York, McGraw-Hill, 1994, pp 155–189
3. Haake R, Schlichtig R, Ullstad DR, et al: Barotrauma: Pathophysiology, risk factors and prevention. *Chest*.1987; 91:608–612

4. Tremblay L, Valenza F, Ribeiro P, et al: Injurious ventilatory strategies increase cytokines and c-fos m-RNA expression in an isolated rat lung model. *J Clin Invest* 1997; 99:944–952
5. Neumann P, Berglund JE, Mondejar E, et al: Dynamics of lung collapse and recruitment during prolonged breathing in porcine lung injury. *J Appl Physiol* 1998; 85:1533–1543
6. Neumann P, Berglund J, Mondejar E, et al: Effect of different pressure levels on the dynamics of lung collapse and recruitment in oleic-acid-induced lung injury. *Am J Respir Crit Care Med* 1998; 158:1636–1643
7. Taskar V, John J, Evander E, et al: Surfactant dysfunction makes lungs vulnerable to repetitive collapse and reexpansion. *Am J Respir Crit Care Med* 1997; 155:313–320
8. Gattinoni L, Pelosi P, Suter P, et al: Acute respiratory distress syndrome caused by pulmonary and extrapulmonary disease. *Am J Respir Crit Care Med* 1998; 158:3–11
9. Carney DE, Bredenberg CE, Schiller HJ, et al: The mechanism of lung volume change during mechanical ventilation. *Am J Respir Crit Care Med* 1999; 160:1697–1702
10. Nieman GF, Bredenberg CE, Clark WR, et al: Alveolar function following surfactant deactivation. *J Appl Physiol Respir Environ Exerc Physiol* 1981; 51:895–904
11. Olkin DM, Joannides M: Capillaroscopic appearance of the pulmonary alveoli in the living dog. *Anat Rec* 1930; 45:121–127
12. Moreci AP, Norman JC: Measurement of alveolar sac diameter by incident-light photomicrography. *Ann Thorac Surg* 1973; 15: 179–186
13. Daly BD, Parks GE, Edmonds CE, et al: Dynamic alveolar mechanics as studied by videomicroscopy. *Respir Physiol* 1975; 24: 217–232
14. Nieman GF, Hakim TS, Bredenberg CE: Effect of increased alveolar surface tension on segmental pulmonary vascular resistance. *J Appl Physiol* 1988; 64:154–161
15. Nieman GF, Bredenberg CE: High surface tension pulmonary edema induced by detergent aerosol. *J Appl Physiol* 1985; 58: 129–136
16. Lutz CJ, Carney DE, Picone AL, et al: Videomicroscopy provides accurate *in vivo* assessment of pulmonary microvascular reactivity in rabbits. *Shock* 1999; 11:367–371
17. McCann UG, Schiller HJ, Carney DE, et al: Supra-physiologic tidal volumes do not cause alveolar over-distention in surfactant deficient lungs. *FASEB J* 1999; 13:A820
18. Wilson TA, Bachofen H: A model for mechanical structure of the alveolar duct. *J Appl Physiol Respir Environ Exerc Physiol* 1982; 52:1064–1070
19. McCann UG, Schiller HJ, Carney DE, et al: Alveolar recruitment as a mechanism of normal lung volume change: Evidence from a novel nuclear imaging technique. *Surgical Forum* 1999; 50:155–157
20. Mead J, Takishima T, Leith D: Stress distri-

bution in lungs: A model of pulmonary elasticity. *J Appl Physiol* 1970; 28:596–608

21. Amato MMP, Barbas C, Medeiros D, et al: Beneficial effects of the “open lung approach” with low distending pressures in acute respiratory distress syndrome. *Am J Respir Crit Care Med* 1995; 152:1835–1846
22. Hickling KG: The pressure-volume curve is greatly modified by recruitment. A mathematical model of ARDS lungs. *Am J Respir Crit Care Med* 1998; 158:194–202

CALCULATION APPENDIX

Based on the collected data, the following calculations were performed on the Baxter Explorer cardiac output computer. Venous admixture was calculated utilizing the following equation:

$$\text{Venous admixture } (Q_s/Q_t) = \frac{100 \cdot [(\text{Hgb} \cdot 1.38) + (0.0031 \cdot \text{PaO}_2) - \text{CaO}_2]}{[(\text{Hgb} \cdot 1.38) + (0.0031 \cdot \text{PaO}_2) - \text{CvO}_2]}$$

where Hgb is hemoglobin, CaO_2 and CvO_2 are arterial and venous blood oxygen content, Q_s is venous admixture blood flow, Q_t is total blood flow, and PaO_2 is the partial pressure of alveolar oxygen. CaO_2 , CvO_2 , and PaO_2 were calculated using the following equations:

$$\begin{aligned} \text{CaO}_2 &= (0.0138 \cdot \text{Hgb} \cdot \text{SaO}_2) \\ &+ 0.0031 \cdot \text{PaO}_2 \\ \text{CvO}_2 &= (0.0138 \cdot \text{Hgb} \cdot \text{SvO}_2) \\ &+ 0.0031 \cdot \text{PaO}_2 \\ \text{PaO}_2 &= [(\text{Pbar} - \text{PH}_2\text{O}) \cdot \text{FIO}_2] \\ &- \text{PaCO}_2 \cdot [\text{FIO}_2 + (1 - \text{FIO}_2) \div 0.8] \end{aligned}$$

where SaO_2 is the measured arterial oxygen saturation (%), SvO_2 is the venous oxygen saturation (%), PaO_2 and PvO_2 are arterial and venous oxygen partial pressure (mm Hg), respectively, FIO_2 is the fraction of inspired oxygen (%), Pbar is the barometric pressure (mm Hg), and PH_2O is the partial pressure of water (mm Hg).

Pulmonary vascular resistance (PVR) was calculated utilizing the following equation:

$$\begin{aligned} \text{PVR (dyne} \cdot \text{sec/cm}^5) \\ &= 80 \cdot (\text{Ppa} - \text{Ppw}) / \text{CO} \end{aligned}$$

where Ppa is mean pulmonary artery pressure (mm Hg), Ppw is pulmonary artery wedge pressure (mm Hg), and CO is cardiac output (L/min).